Synthesis and Characterization of Sunflower Oil-Based Polysulfide Polymer/Cloisite 30B Nanocomposites

Moqadam, Samira; Salami-Kalajahi, Mehdi*[+]

Department of Polymer Engineering, Sahand University of Technology, P.O. Box 51335-1996, Tabriz, I.R. IRAN

Mahdavian, Mohammad

Department of Surface Coating and Corrosion, Institute for Color Science and Technology, P.O. Box 16765-654, Tehran, I.R. IRAN

ABSTRACT: *In current work, halogenated sunflower oil was reacted with Na_2S_3 to produce sunflower oil-based polysulfide polymer. Cloisite 30B as organomodified nanoclay was used in different contents to investigate its effect on the properties of the synthesized polymer. All nanocomposites were prepared via in situ polymerization method in aqueous media. Fourier Transform-InfraRed (FT-IR) spectroscopy revealed the inclusion of nanoclay in a polymeric matrix. X-Ray Diffraction (XRD) and Transmission Electron Microscopy (TEM) were used to study the degree of intercalation/exfoliation of nanoplatelets in matrices. Proton Nuclear Magnetic Resonance (^{1}H NMR) was utilized to study the molecular weight of synthesized polymers. Thermal stability of nanocomposites was determined by means of Thermal Gravimetric Analysis (TGA) and Differential Scanning Calorimetry (DSC) was used to investigate thermophysical properties. According to results, nanocomposite with 1 wt. % of Cloisite 30B showed an exfoliated morphology whereas the higher amount of nanoclay resulted in intercalated nanoplatelets with different degrees of intercalation. Also, adding more Cloisite 30B nanoplatelets led to more decrease in molecular weight. After the introduction of nanoclay into nanocomposites structure and increasing its content, the thermal stability of nanocomposites was improved whereas no significant improvement of thermal stability was observed by increasing clay content from 3 to 5 wt. %. Also, all samples showed only the glass transition temperature (T_g) and no distinct peak related to melting was observed. Adding more nanoclay resulted in higher T_g value due to the confinement effect of nanoplatelets.*

KEYWORDS: *Polysulfide polymer; Sunflower oil; Nanocomposites; Cloisite 30B.*

INTRODUCTION

Polysulfide polymers are widely used in different applications such as adhesives, sealants, etc. [1-2]. They are commonly produced by the polymerization of short-chain dichlorohydrocarbons with aqueous sodium

** To whom correspondence should be addressed.*
+ E-mail: m.salami@sut.ac.ir
1021-9986/2018/1/185-192 8/$/5.08
DOI:

polysulfide [3]. Equation (1) states the general polycondensation mechanism to produce polysulfide polymers.

$$n\ (Cl-R-Cl)\ +\ n(Na_2S_x)\ \rightarrow \quad (1)$$
$$[-RS_x-]_n + 2n\ NaCl$$

Polysulfide polymers with polysulfide linkages in their structure show rubbery behavior with low thermal stability [4]. In this field, fabrication of their nanocomposites with different nanoparticles including clay nanoplatelets [5], titanium dioxide nanoparticles [6], carbon nanotubes [7] and graphene nanosheets [8] has been applied to improve thermophysical properties of polysulfide polymers. Among different nanoparticles, relatively low loadings of clay nanoplatelets result in significant improvements in mechanical properties [9] and thermal stability [10-11] of polymer matrices. Additionally, dispersion quality of clay platelets in matrix severely affects the aforementioned properties [12]. Due to a variety of polymerization systems and methods, in situ polymerization is one of the most interesting techniques for nanocomposite preparation where a high degree of dispersion of nanoparticles can be achieved [13].

Recently, a new class of polysulfide polymers based on sunflower oil has been introduced [14] in which double bonds of sunflower oil are halogenated to give polyhalide. Polymerization of halogenated oil with disodium polysulfide yields sunflower oil-based polysulfide polymer. However, similar to other polysulfide polymers, sunflower oil-based polysulfide polymer shows low thermal stability. In this work, an effort was made to synthesize sunflower oil-based polysulfide polymer/Cloisite 30B nanocomposites by in situ polymerization. The effects of the amount of nanofiller on the properties of the nanocomposites were investigated. The molecular weight was monitored via proton Nuclear Magnetic Resonance (^{1}H NMR). Structural and morphological characteristics of the nanocomposites were studied by X-Ray Diffraction (XRD) and Transmission Electron Microscopy (TEM) analyses. Also, the thermophysical properties of nanocomposites were investigated by Thermal Gravimetric Analysis (TGA) and Differential Scanning Calorimetry (DSC).

EXPERIMENTAL SECTION

Materials

Benzoyl peroxide (BPO, 75%, Merck, Darmstadt, Germany) was purified via recrystallization from methanol. Sunflower oil was supplied by FRICO, Tehran, Iran. Aqueous hydrochloric acid (HCl, 37%, Mojallali, Tehran, Iran), calcium chloride ($CaCl_2$, 97%, Mojallali, Tehran, Iran), sodium hydroxide (NaOH, 97%, Mojallali, Tehran, Iran), sulfur (S, 99%, Merck, Darmstadt, Germany) and Cloisite 30B (montmorillonite that goes through an ion-exchanged reaction with methyl tallowbis-2-hydroxyethyl quaternary ammonium surfactant, Southern Clay Products, Gonzales, TX) was used as received.

Preparation of Polysulfide/Clay Nanocomposites

Halogenated oil and Na_2S_3 were synthesized according to previously described methods [14]. At first, BPO (1.0 g, 4.1 mmol) was added to $CaCl_2$-dried sunflower oil (100 mL, 104.4 mmol) and the mixture was stirred for 10 min at 70 °C. Then, the mixture was placed in an ice-water bath and HCl vapor was purged into the reactor for 5 h. Finally, halogenated oil was filtered via 0.2 μm-pore size nitrocellulose membrane filters and dried in a vacuum oven at 50 °C overnight. To prepare Na_2S_3, NaOH (10.0 g, 311.9 mmol) was dissolved in water (100 mL) at room temperature. After addition of sulfur (11.371 g, 363.9 mmol), the mixture was stirred for 24 h at room temperature to make a homogeneous orange-colored solution. To synthesize nanocomposites, Cloisite 30B was dispersed in an aqueous solution of Na_2S_3 via 30-min sonication at room temperature. After increasing temperature to 70 °C, 20 mL of halogenated oil was added slowly and the reaction was continued for 24 h at 100 °C. Finally, the product was washed with water to remove NaCl salt and subsequently by HCl to reduce the pH to 5. Final products were dried in a vacuum oven at 50 °C overnight. The content of Cloisite 30B was considered 0, 1, 3 and 5 wt. % with respect to halogenated oil and nanocomposites were named P0, P1, P3, and P5 respectively. Scheme 1 shows the synthetic route to prepare above-mentioned nanocomposites.

Separation of polymer chains from clay platelets

The prepared nanocomposites were dissolved in chloroform. By high-speed ultracentrifugation (10000 rpm) and then passing the solution through a 0.2 μm regenerated cellulose (RC) filter, free polymer chains were separated from nanoclays. Finally, polymer chains were dried overnight in a vacuum oven at 50 °C.

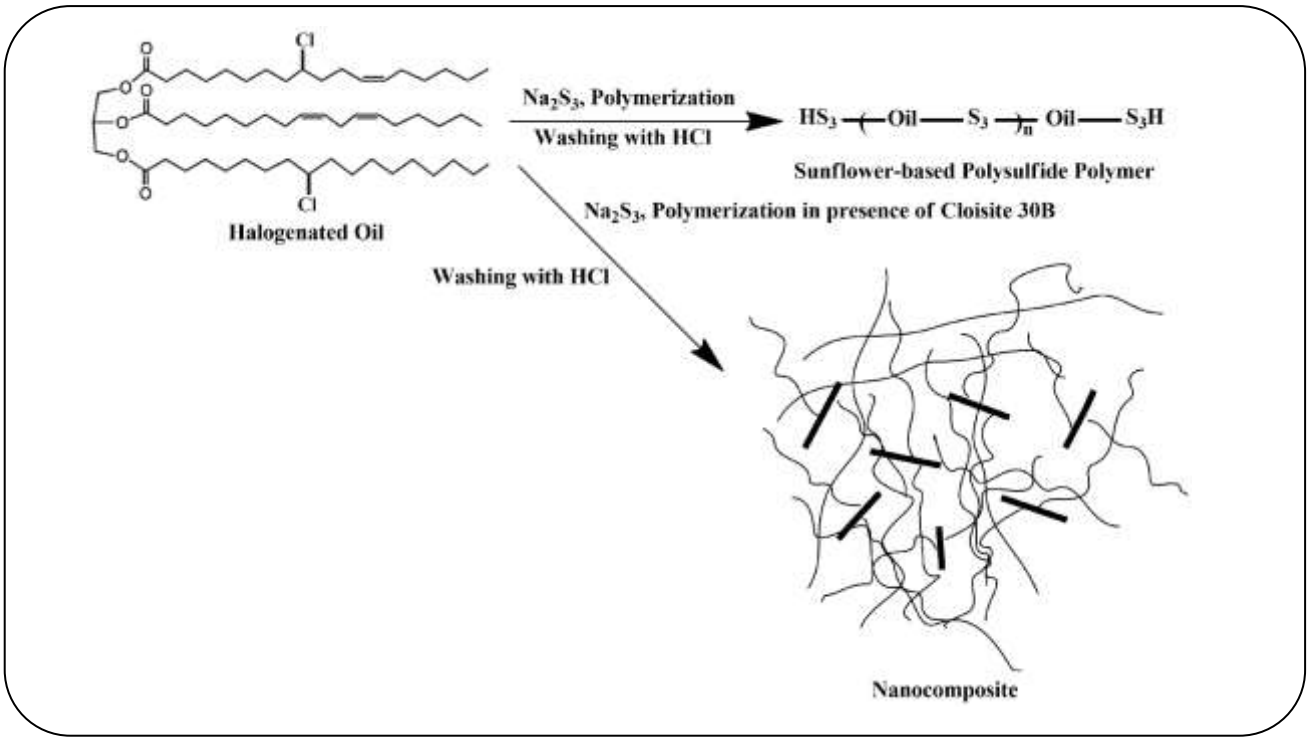

Scheme 1: Synthetic route to prepare polysulfide polymer/clay nanocomposite.

Instrumentation

FT-IR spectra were recorded on a Bomem FT-IR spectrophotometer, within a range of 500-4000 cm^{-1} using a resolution of 4 cm^{-1}. An average of 32 scans has been reported for each sample. Cell pathlength was kept constant during all the experiments. The samples were prepared on a KBr pellet in vacuum desiccators under a pressure of 0.01 Torr. X-Ray Diffraction (XRD) spectra were collected on an X-ray diffraction instrument (Siemens D5000) with a Cu target (λ = 0.1540 nm) at room temperature. The system consists of a rotating anode generator which operated at 35 kV and 20 mA. The samples were scanned from 2θ = 2 to 10 ° at the step scan mode; the diffraction pattern was recorded using a scintillation counter detector. Transmission Electron Microscope (TEM), Philips EM208, with an accelerating voltage of 120 kV was used to study the morphology of the nanocomposites; the samples of 70 nm thickness were prepared by Reichert ultramicrotome (type OMU 3). Thermal gravimetric analyses were carried out with a PL thermo-gravimetric analyzer (Polymer Laboratories, TGA 1000, UK). The thermograms were obtained from ambient temperature to 600 °C at a heating rate of 10 °C/min. A sample weight of about 10 mg was used for all the measurements and nitrogen were used as the purging gas at a flow rate of 50 mL/min. Differential scanning calorimetry was carried out using a DSC instrument (NETZSCH DSC 200 F3, Netzsch Co., Bavaria, Germany). Nitrogen at a rate of 50 mL/min was used as the purging gas. Aluminum pans containing 3 mg of sample were sealed using the DSC sample press. The sample was heated from -20°C to 180°C at a heating rate of 10 °C/min. T_g was obtained as the inflection point of the heat capacity jump.

RESULTS AND DISCUSSION

To confirm the incorporation of Cloisite 30B into the polymer matrix, FT-IR spectra of Cloisite 30B, P0 and P1 are shown in Fig. 1. In all spectra, characteristic peaks at 2930 and 2850 cm^{-1} are related to the asymmetric and symmetric stretching vibration of C-H bonds respectively [15-16]. Also, =C-H bonds show a stretching vibration at 3010 cm^{-1} in P0 and P1 samples and an out-of-plane stretching vibration at 915 cm^{-1} in all spectra [17]. Vibration peak at 1750 cm^{-1} is ascribed to carbonyl groups of oil structure [18] and stretching vibrations of C=C bonds are observed at 1655 cm^{-1}. Scissoring and bending vibrations of $-CH_2-$ appears at 1465 and 725 cm^{-1} respectively.

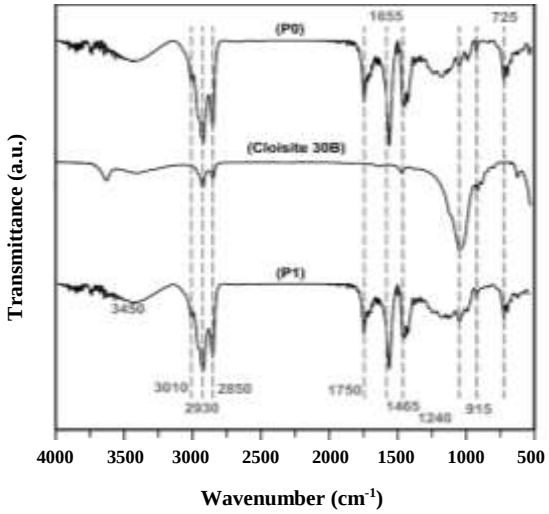

Fig. 1: FT-IR spectra of Cloisite 30B, P0, and P1.

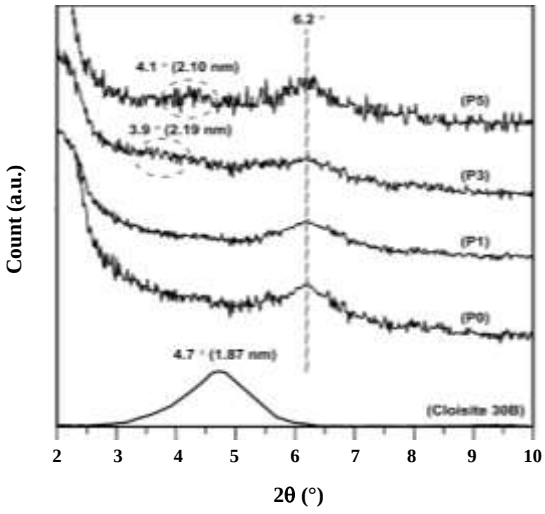

Fig. 2: XRD patterns of Cloisite 30B, neat polysulfide and prepared nanocomposites.

The characteristic peak at 1050 cm^{-1} in Cloisite 30B and P1 samples are ascribed to vibration of Si-O-Si bonds of the octahedral nanoplatelets of clay structure [19]. As a result, this peak in P1 is much broader than P0 sample. These results show that nanoplatelets are incorporated in the polymeric matrix successfully.

XRD analysis was used to study the dispersion of nanoplatelets in polymeric matrices. Fig. 2 shows the XRD patterns of Cloisite 30B, neat polymer (P0) and all nanocomposites in diffraction angles of 2θ = 2–10°. Cloisite 30B shows a diffraction peak at 2θ = 4.7° with a basal distance of 1.87 nm due to (001) basal plane (d_{001}) [20]. Morphology of nanoplatelets/polymer nanocomposites is categorized in several ways including immiscible, intercalated, partially exfoliated, and exfoliated [21]. Such a morphology is affected by nanoplatelets content, chemical nature of the surface, and synthesis method. Generally, exfoliation occurs in low nanofiller contents with appropriate surface nature whereas higher nanoparticle contents result in intercalated morphology. Cloisite 30B contains some hydroxyl groups on its surface those can interact with ester moieties of sunflower oil-based polysulfide polymer. Accordingly, no obvious peak related to Cloisite 30B is observed in P1 whereas P3 and P5 show a weak peak at 2θ = 3.9 (d-spacing = 2.19 nm) and 4.1 ° (2.10 nm) respectively. Combining these results with images obtained from TEM shows that P1 nanocomposite has an exfoliated morphology whereas P3 and P5 contain intercalated nanoplatelets with different intercalation degrees. Forasmuch as there is no difference between interactions of matrices with nanoplatelets in prepared nanocomposites, nanofiller content is the most important parameter that affects the morphology of samples. In the case of the content of nanofiller, higher filler content results in a lower degree of exfoliation and commonly occurring intercalation of nanoplatelets [22]. Also, neat polysulfide polymer and all nanocomposites show a very broad peak with the climax of 6.2 ° that may be attributed to the amorphous structure of samples containing polysulfide moieties.

^{1}H NMR analysis was carried out in $CDCl_3$ for all samples after separation of clay nanoplatelets where characteristic signals of all samples were same except their area of peaks. The characteristic signals of synthesized polymers were as follow: δ((CH$_2$)$_n$C**H**$_3$) = 0.86-0.89 ppm, δ((C**H**$_2$)$_n$) = 1.25-1.31 ppm, δ(CH=CHC**H**$_2$(CH$_2$)$_n$, C**H**S$_x$, CHS$_x$C**H**$_2$) = 2.00-2.08 ppm, δ(CH=CHC**H**$_2$CH=CH) = 2.75-2.79 ppm, δ(COOC**H**$_2$(CH$_2$)$_n$) = 2.29-2.33 ppm, δ(C**H**=C**H**) = 5.29-5.39 ppm, δ(C**H**$_2$-OCO and C**H**-OCO) = 4.15-4.29 ppm, δ(–S-S**H**) = 2.42 and δ(–S-S-S**H**) = 2.54 [14, 23]. Results from ^{1}H NMR were used to calculate the molecular weight of samples according to Equation (2):

$$M_n = \frac{A(-CH_3-)/9}{A(-S_xH)/2} \times MW_{\text{repeating unit}} + MW_{-S_xH} \quad (2)$$

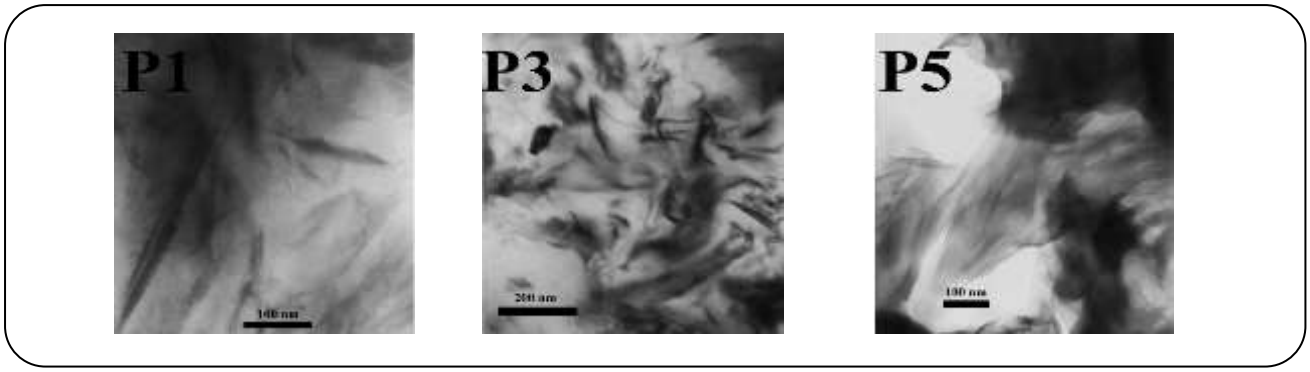

Fig. 3: TEM image of P1, P3, and P5.

Where A means the surface area of the related peak, $MW_{repeating\ unite}$ is the molecular weight of oil as a repeating unit and $MW_{\text{-SxH}}$ is the molecular weight of end groups. A(-CH_3-) is divided by 9 due to the presence of 9 -CH_3- proton atoms in oil structure and A(-SxH-) is divided by 2 because of two thiolic end groups. The peak area ratio of CH_3 protons to thiolic protons corresponds to a molecular weight of 8800, 8370, 7730 and 7560 g/mol for P0, P1, P3, and P5 respectively. Results show that adding more Cloisite 30B nanoplatelets results in a decrease of molecular weight slightly.

Thermal stability of samples was investigated by TGA as depicted in Fig. 4. All samples showed two stages of degradation. The first stage of degradation is ascribed to the degradation of oxygen-containing groups [24-25] of oil structure which takes place between 190 and 240 °C in P0 sample. However, by loading Cloisite 30B and increasing its content in nanocomposite composition, the degradation temperature of first stage increases due to nanoclay-induced thermal stability. Also, the weight loss of samples decreases in the first stage of degradation as the content of nanoclay increases. The second and main stage of degradation is related to the random chain scission that occurs between 250 and 313 °C with $T_{d,max}$ = 296 °C for P0 sample. This Low thermal stability of the neat polymer is related to weak C-S bonds, aliphatic carbon structure and low molecular weight [26-28]. After the introduction of nanoclay into nanocomposites structure and increasing its content, thermal stability of nanocomposites becomes better. Accordingly, $T_{0.1}$ and $T_{0.5}$ (temperatures of 10 and 50 wt. % of mass loss) increase whereas P5 shows the highest improvement of thermal stability. Although nanoclay content has a significant effect on the thermal stability of nanocomposites, results show that there is no significant improvement of thermal stability by increasing clay content from 3 to 5 wt. %. Considering the molecular weight of the matrix, the higher molecular weight of polymers results in higher thermal stability [29]. According to ^{1}H NMR results, the neat polymer has higher molecular weight and higher content of Cloisite 30B leads to the lower molecular weight of the matrix. Thus, the low molecular weight of the matrix in a higher content of Cloisite 30B results in less improvement of thermal stability. Also, the origin of improvement of thermal stability is the ability of layered nanoparticles to obstruct the volatile gas produced by thermal decomposition. According to "barrier model" [30], thermal decomposition commences from the surface of nanocomposites and leads to an increase in the content of nanosheets and formation of a protective layer by nanosheets. Also, according to nanoconfinement theory [31], newly formed radicals derived from the degradation of the polymer are confined by platelets followed by a variety of bimolecular reactions. As degradation progresses, nanoplatelets migrate gradually to the surface and form a barrier due decrease in surface free energy.

The thermophysical properties and thermal transitions of all samples were investigated by DSC under a nitrogen atmosphere as shown in Fig. 5. Each sample was initially heated from ambient temperature to 180 °C in order to remove residual volatile components and thermal history. Then, all samples were cooled to -20 °C at the cooling rate of 10 °C/min, followed by heating from -20 to 180 °C at the same heating rate. According to results, all samples showed only glass transition temperature (T_g) and no distinct peak related to melting was observed. This predicates that all samples have an amorphous structure and inclusion of nanoclay does not change the structure

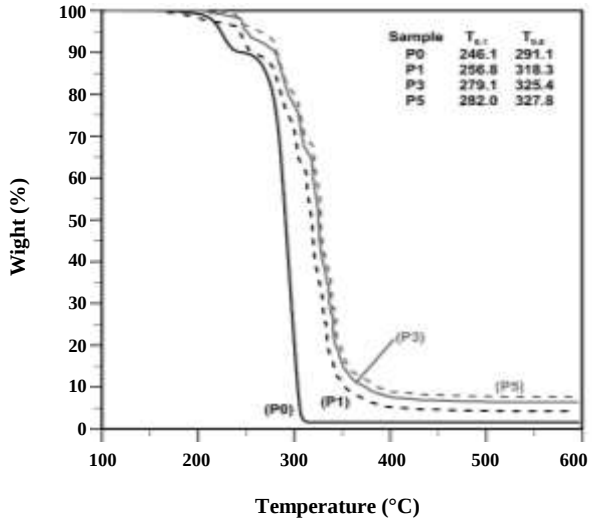

Fig. 4: TGA thermograms of neat polysulfide polymer (P0) and P1, P3 and P5 nanocomposites.

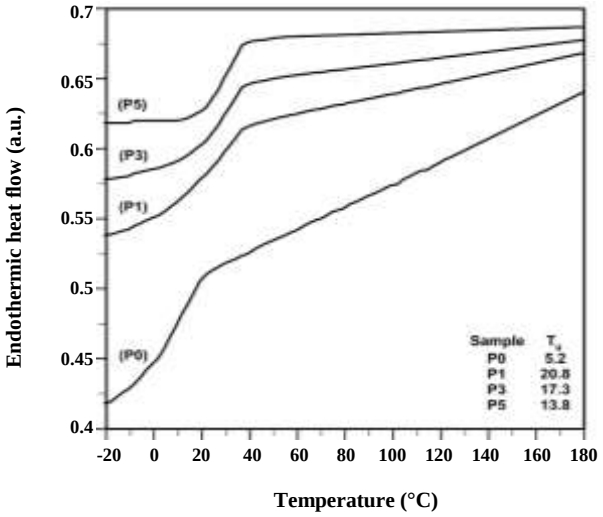

Fig. 5: DSC curves of neat polysulfide polymer (P0) and P1, P3 and P5 nanocomposites.

of polysulfide polymer except for its molecular weight as proved by ^{1}H NMR results. The backbone structure of synthesized polysulfide polymer and soft C–S and S–S linkages are the main reasons those prevent the formation of crystalline structure [32]. The effect of chain confinement due to nanoplatelets steric hindrance was evaluated

by comparing T_g values of neat polysulfide polymer and nanocomposites. Adding nanoclay results in higher T_g value compared to neat polymer due to the confinement effect of nanoplatelets. The rigid two-dimensional platelets exert a confinement on the steric mobility of chains, and hence the motions of molecule segments, which causes higher T_g values [33]. However, more clay content results in intercalation

CONCLUSIONS

A number of batch experiments were carried out to synthesize sunflower oil-based polysulfide polymer/Cloisite 30B nanocomposites via interfacial condensation polymerization. Different amounts of Cloisite 30B were used to investigate the effects of clay content on the properties of nanocomposites. ^{1}H NMR results showed that Cloisite 30B nanoplatelets led to a decrease in molecular weight due to depression of chains' diffusion and hindrance effect of nanoclay. The nanocomposite with 1 wt. % of Cloisite 30B showed no characteristic peak in XRD. Additionally, TEM micrographs of nanocomposites demonstrated that exfoliated structure has been obtained for P1 and nanocomposites with a higher amount of nanoclay had intercalated morphology. TGA results showed that thermal stabilities of all the nanocomposites were higher than the neat polymer whereas the improvement of thermal stability was related to the molecular weight of matrix and thermal stability of the nanosheets. According to DSC results, all samples exhibited only glass temperature and no distinct T_m was observed for samples. These results showed that amorphous structure is more predominant in all samples. Also, adding nanoplatelets resulted in higher T_g values compared to neat polymer due to the confinement effect of nanoparticles. However, when the content of nanoclay increases, dueto intercalation of nanoclays instead of exfoliation, nanoclays play an insufficient role to improve thermophysical properties and results in lower T_g compared to P1 sample.

Received: Aug. 22, 2016; Accepted: Jun. 12, 2017

REFERENCES

[1] Farajpour T., Bayat Y., Keshavarz M. H., Zanjirian E., Investigating the Effect of Modifier Chain Length on Insulation Properties of Polysulfide Modified Epoxy Resin, *Iran. J. Chem. Chem. Eng. (IJCCE)*, **33** (1): 37-44 (2014).

[2] Abdouss M., Farajpour T., Derakhshani M., The Effect of Epoxy-Polysulfide Copolymer Curing Methods on Mechanical-Dynamical and Morphological Properties, *Iran. J. Chem. Chem. Eng. (IJCCE)*, **30** (4): 37-44 (2011).

[3] Kariminejad B., Salami-Kalajahi M., Roghani-Mamaqani H., Thermophysical Behaviour of Matrix-Grafted Graphene/poly(Ethylene Tetrasulphide) Nanocomposites, *RSC Adv*., **5**(121): 100369-100377 (2015).
DOI: https://doi.org/10.1039/C5RA20254J.

[4] Allahbakhsh A., Sheydaei M., Mazinani S., Kalaee M., Enhanced Thermal Properties of Poly(ethylene tetrasulfide) via Expanded Graphite Incorporation by in Situ Polymerization Method, *High Perform. Polym.*, **25**(5): 576-583 (2013).
DOI: https://doi.org/10.1177/0954008313476314.

[5] Zou H., Xu W., Zhang Q., Fu Q., Effect of Alkylammonium Salt on the Dispersion and Properties of Poly(p-phenylene sulfide)/Clay Nanocomposites via Melt Intercalation, *J. Appl. Polym. Sci*., **99**(4): 1724-1731 (2006).
DOI: https://doi.org/10.1002/app.22690.

[6] Bahadur S., Sunkara C., Effect of Transfer Film Structure, Composition and Bonding on the Tribological Behavior of Polyphenylene Sulfide Filled with Nano Particles of TiO_2, ZnO, CuO and SiC, *Wear*, **258**(9): 1411-1421 (2005).
DOI: https://doi.org/10.1016/j.wear.2004.08.009.

[7] Han S.-C., Song M.-S., Lee H., Kim H.-S., Ahn H.-J., Lee J.-Y., Effect of Multiwalled Carbon Nanotubes on Electrochemical Properties of Lithium/Sulfur Rechargeable Batteries, *J. Electrochem. Soc*., **150**(7): A889-A893 (2003).
DOI: https://doi.org/10.1149/1.1576766.

[8] Kariminejad B., Salami-Kalajahi M., Roghani-Mamaqani H., Noparvar-Qarebagh A., Effect of Surface Chemistry of Graphene and Its Content on the Properties of Ethylene Dichloride- and Disodium Tetrasulfide-Based Polysulfide Polymer Nanocomposites, *Polym. Compos*., **38**(S1): E515-E524 (2017).
DOI: https://doi.org/10.1002/pc.23857.

[9] Rahimi-Razin S., Salami-Kalajahi M., Haddadi-Asl V., Roghani-Mamaqani H., Effect of Different Modified Nanoclays on the Kinetics of Preparation and Properties of Polymer-based Nanocomposites, *J. Polym. Res*., **19**(9): 9954 (2012).
DOI: https://doi.org/10.1007/s10965-012-9954-x.

[10] Ahmadian-Alam L., Haddadi-Asl V., Hatami L., Roghani-Mamaqani H., Salami-Kalajahi M., Kinetic Study of In Situ Normal and AGET Atom Transfer Radical Copolymerization of n-butyl Acrylate and Styrene: Effect of Nanoclay Loading and Catalyst Concentration, *Int. J. Chem. Kinet*., **44** (12), 789-799 (2012).
DOI: https://doi.org/10.1002/kin.20729.

[11] Khezri Kh., Haddadi-Asl V., Roghani-Mamaqani H., Salami-Kalajahi M., Nanoclay Encapsulated Polystyrene Microspheres by Reverse Atom Transfer Radical Polymerization, *Polym. Compos*., **33**(6): 990-998 (2012).
DOI: https://doi.org/10.1002/pc.22233.

[12] Khezri Kh., Haddadi-Asl V., Roghani-Mamaqani H., Salami-Kalajahi M., Polystyrene-Organoclay Nanocomposites Produced by in situ Activators Regenerated by Electron Transfer for Atom Transfer Radical Polymerization, *J. Polym. Eng*., **32**(4-5): 235-243 (2012).
DOI: https://doi.org/10.1515/polyeng-2012-0029.

[13] Torkpur-Biglarianzadeh M., Salami-Kalajahi M., Multilayer Fluorescent Magnetic Nanoparticles with Dual Thermoresponsive and pH-sensitive Polymeric Nanolayers as Anti-cancer Drug Carriers, *RSC Adv*., **5** (38), 29653-29662 (2015).
DOI: https://doi.org/10.1039/C5RA01444A.

[14] Moqadam S., Salami-Kalajahi M., Halogenated Sunflower Oil as a Precursor for Synthesis of Polysulfide Polymer, *e-Polymers*, **16**(1): 33-39 (2016).
DOI: https://doi.org/10.1515/epoly-2015-0152.

[15] Nikdel M., Salami-Kalajahi M., Salami Hosseini M., Synthesis of Poly(2-hydroxyethyl Methacrylate-co-acrylic acid)-Grafted Graphene Oxide Nanosheets via Reversible Addition–Fragmentation Chain Transfer Polymerization, *RSC Adv*., **4**(32): 16743-16750 (2014).
DOI: https://doi.org/10.1039/C4RA01701C.

[16] Amirshaqaqi N., Salami-Kalajahi M., Mahdavian M., Investigation of corrosion behavior of aluminum flakes coated by polymeric nanolayer: Effect of polymer type, *Corros. Sci*., **87**: 392-396 (2014).
DOI: https://doi.org/10.1016/j.corsci.2014.06.045.

[17] Sarsabili M., Parvini M., Salami-Kalajahi M., Ganjeh-Anzabi P., In Situ Reversible Addition–Fragmentation Chain Transfer Polymerization of Styrene in the Presence of MCM-41 Nanoparticles: Comparing "Grafting from" and "Grafting through" Approaches, *Adv. Polym. Technol*., **32**(4): 21372 (2013).
DOI: https://doi.org/10.1002/adv.21372.

[18] Nikdel M., Salami-Kalajahi M., Salami Hosseini M., Dual thermo- and pH-sensitive Poly(2-hydroxyethyl methacrylate-co-acrylic acid)-grafted Graphene Oxide, *Colloid Polym. Sci*., **292**(10): 2599-2610 (2014).
DOI: https://doi.org/10.1007/s00396-014-3313-x.

[19] Roghani-Mamaqani H., Haddadi-Asl V., Najafi M., Salami-Kalajahi M., Well-defined Nanofiberous Polystyrene Nanocomposites with Twofold Chains by ATRP, *Polym. Sci. Ser. B*, **54**(3-4): 153-160 (2012).
DOI: https://doi.org/10.1134/S1560090412030074.

[20] Roghani-Mamaqani H., Haddadi-Asl V., Najafi M., Salami-Kalajahi M., Evaluation of the Confinement Effect of Nanoclay on the Kinetics of Styrene Atom Transfer Radical Polymerization, *J. Appl. Polym. Sci*., **123**(1): 409-417 (2012).
DOI: https://doi.org/10.1002/app.34511.

[21] Khezri Kh., Haddadi-Asl V., Roghani-Mamaqani H., Salami-Kalajahi M., Synthesis of Well-defined Clay Encapsulated Poly (Styrene-co- Butyl acrylate) Nanocomposite Latexes via Reverse Atom Transfer Radical Polymerization in Miniemulsion, *J. Polym. Eng*., **32**(2): 111-119 (2012).
DOI: https://doi.org/10.1515/polyeng-2011-0149.

[22] Tajeddin B., Ramedani N., Preparation and Characterization (Mechanical and Water Absorption Properties) of CMC/PVA/Clay Nanocomposite Films, *Iran. J. Chem. Chem. Eng. (IJCCE)*, **35** (3): 9-15 (2016).

[23] Argyropoulos D. S., Hou Y., Ganesaratnam R., Harpp D. N., Koda K., Quantitative ^{1}H NMR Analysis of Alkaline Polysulfide Solutions, *Holzforschung*, **59**(2): 124-131 (2005).
DOI: https://doi.org/10.1515/HF.2005.019.

[24] Salami-Kalajahi M., Haddadi-Asl V., Behboodi-Sadabad F., Rahimi-Razin S., Roghani-Mamaqani H., Effect of Silica Nanoparticle Loading and Surface Modification on the Kinetics of RAFT Polymerization, *J. Polym. Eng*., **32**(1): 13-22 (2012).
DOI: https://doi.org/10.1515/polyeng.2011.601.

[25] Panahian P., Salami-Kalajahi M., Salami Hosseini M., Synthesis of Dual Thermosensitive and pH-Sensitive Hollow Nanospheres Based on Poly(acrylic acid‑b‑2-hydroxyethyl methacrylate) via an Atom Transfer Reversible Addition-Fragmentation Radical Process, *Ind. Eng. Chem. Res*., **53**(19): 8079-8086 (2014).
DOI: https://doi.org/10.1021/ie500892b.

[26] Rahimi-Razin S., Haddadi-Asl V., Salami-Kalajahi M., Behboodi-Sadabad F., Roghani-Mamaqani H., Properties of Matrix-grafted Multi-Walled Carbon Nanotube/Poly(methyl methacrylate) Nanocomposites Synthesized by In Situ Reversible Addition-Fragmentation Chain Transfer Polymerization, *J. Iran. Chem. Soc*., **9**(6): 877-887 (2012).
DOI: https://doi.org/10.1007/s13738-012-0104-5.

[27] Amirshaqaqi N., Salami-Kalajahi M., Mahdavian M., Corrosion Behavior of Aluminum/Silica/Polystyrene Nanostructured Hybrid Fakes, *Iran. Polym. J.*, **23**(9): 699-706.
DOI: https://doi.org/10.1007/s13726-014-0264-5.

[28] Jahanmardi R., Eslami B., Tamaddon H., Effects of Nanoclay on Cellular Morphology and Water Absorption Capacity of Poly(vinyl alcohol) Foam, *Iran. J. Chem. Chem. Eng. (IJCCE), (*2017), accepted.

[29] Salami-Kalajahi M., Haddadi-Asl V., Rahimi-Razin S., Behboodi-Sadabad F., Roghani-Mamaqani H., Najafi M., Effect of Loading and Surface Modification of Nanoparticles on the Properties of PMMA/Silica Nanocomposites Prepared via In situ Free Radical Polymerization, *Int. J. Polym. Mater*., **62**(6): 336-344 (2013).
DOI: http://dx.doi.org/10.1080/00914037.2012.670826.

[30] Hatami L., Haddadi-Asl V., Roghani-Mamaqani H., Ahmadian-Alam L., Salami-Kalajahi M., Synthesis and Characterization of Poly (styrene-co-butyl acrylate)/clay Nanocomposite Latexes in Miniemulsion by AGET ATRP, *Polym. Compos*., **32**(6): 967-975 (2011).
DOI: https://doi.org/10.1002/pc.21115.

[31] Khezri K., Haddadi-Asl V., Roghani-Mamaqani H., Salami-Kalajahi M., Synthesis and Characterization of Exfoliated Poly (styrene-co-methyl methacrylate) Nanocomposite via Miniemulsion Atom Transfer Radical Polymerization: an Activators Generated by Electron Transfer Approach, *Polym. Compos.*, **32**(12): 1979-1987 (2011).
DOI: https://doi.org/10.1002/pc.21229.

[32] Saeed K., Park S.-Y., Preparation and Properties of Polycaprolactone/Poly (Butylene Terephthalate) Blend, *Iran. J. Chem. Chem. Eng. (IJCCE)*, **29**(3): 77-81 (2010).

[33] Sarsabili M., Parvini M., Salami-Kalajahi M., Asfadeh A., Effect of MCM-41 Nanoparticles on the Kinetics of Free Radical and RAFT Polymerization of Styrene, *Iran. Polym. J*., **22**(3): 155-163 (2013).
DOI: https://doi.org/10.1007/s13726-012-0114-2.